CSIRO PUBLISHING

Publications of the Astronomical Society of Australia, 2008, **25**, 18–29 www.publish.csiro.au/journals/pasa

Nuclear Physics of the *s* Process

I. Dillmann[A], *C. Domingo Pardo*[A], *F. Käppeler*[A,D], *A. Mengoni*[B], *and K. Sonnabend*[C]

[A] Forschungszentrum Karlsruhe, Institut für Kernphysik, D-76021 Karlsruhe, Germany
[B] International Atomic Energy Agency, Nuclear Data Section, P.O. Box 100, A-1400 Vienna, Austria
[C] Institut für Kernphysik, Technische Universität Darmstadt, Schlossgartenstrasse 9, D-64289 Darmstadt, Germany
[D] Corresponding author. Email: franz.kaeppeler@ik.fzk.de

Received 2007 October 10, accepted 2007 November 15

Abstract: Starting from a sketch of the *s*-process concept formulated 50 years ago, the nuclear physics data for *s*-process calculations are briefly reviewed with emphasis on the status of neutron capture cross sections and beta decay rates. Accurate and comprehensive experimental data are mandatory as direct input for *s*-process calculations as well as for improving the complementary information from nuclear theory. The current challenges of the field are discussed in the light of new or optimized methods and state-of-the-art facilities, indicating the potential for accurate measurements and the possibility to study cross sections of radioactive isotopes. These opportunities will be considerably enriched by the enormous improvements provided by new facilities.

1 The *s* Process in Retrospect

Looking back on the founding papers of Nuclear Astrophysics published 50 years ago by Burbidge et al. (1957, hereafter referred to as B^{2}FH) and by Cameron (1957) it is inspiring to see that already the entire *s*-process panorama was sketched in its essential parts. The visionary view of these papers is the more admirable as the basics were still pretty incomplete.

This is certainly also true for the *s* process. In spite of the fact that neither the neutron source reactions nor the neutron capture cross sections in the astrophysically relevant energy range were known apart from some rudimentary information, all essential features had been inferred from these meager information. The product of the stellar (n, γ) cross sections and of the resulting *s* abundances, $\langle\sigma\rangle N_s$, which represents the reaction flow, was found to be a smooth function of mass number A. From the composite slope of this function two different *s* processes were postulated. The steep decline between $A \approx 63$ and 100 was interpreted as the result of an *s*-process site with not enough neutrons available per ^{56}Fe seed to build the nuclei to their saturation abundances. In the mass region beyond $A \approx 100$, the much smaller slope was suggesting that steady flow was achieved and that all of these nuclei reached their saturation abundances. It was concluded that 'the two different processes might have occurred in two different red-giant stars' (Burbidge et al. 1957), completely consistent with what is now called the weak *s* process during core He burning[1,2] and shell C burning (Raiteri et al. 1991, 1993; Limongi et al. 2000) in massive stars on the one hand and the main *s* component contributed by thermally pulsing low mass asymptotic giant branch (AGB) stars (Straniero et al. 1995; Gallino et al. 1998; Arlandini et al. 1999) on the other hand. Eventually, the identification of the *s*-process sites has been shown to be an important ingredient for quantitative studies of galactic chemical evolution (Travaglio et al. 1999, 2001, 2004).

The main difficulty that prevented further conclusions was due to the lack of reliable neutron capture cross sections. In total, the cross sections of only 25 isotopes had been experimentally investigated at that time. Moreover, these data were uncertain by more than a factor of two in a number of cases. All the remaining data were extrapolated from thermal cross sections or from pile reactivity measurements using plausible assumptions on the energy dependence. The importance of a complete set of experimental data for the reliable description of the $\langle\sigma\rangle N_s$-curve is illustrated in Figure 1, which corresponds to the situation obtained by the time of the cross section compilation of Bao et al. (2000), when most of the cross sections had been measured.

Apart from the clear separation of the two *s*-process components, Figure 1 also shows the pronounced effect of *s*-process branchings, which could not be addressed by B^{2}FH simply because the data were far too uncertain to reveal their signatures in the $\langle\sigma\rangle N_s$-curve. These branchings are the result of the competition between neutron capture and β-decay at unstable isotopes in the half-life range from a few months to a few years. For the same reason, also the effect of stellar temperatures on the β-decay half-lives had not been anticipated, that is for the branch point ^{79}Se. The branching at ^{79}Se is characterized by the strongly different $\langle\sigma\rangle N_s$-values of the *s*-only isotopes ^{80}Kr

[1] `http://www.ucolick.org/~alex`
[2] `http://www.mporzio.astro.it/~limongi`

 10.1071/AS07043 1323-3580/08/01018

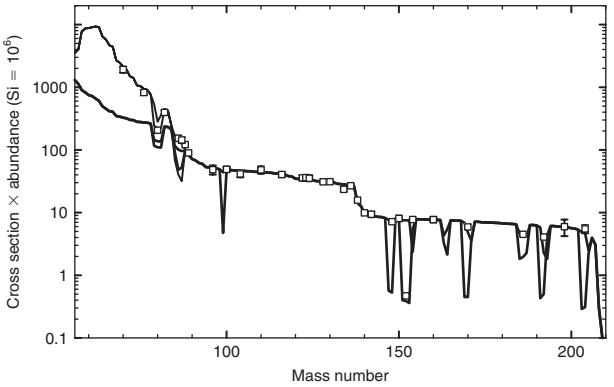

Figure 1 The characteristic product of cross section times *s*-process abundance, $\langle\sigma\rangle N_s$, plotted as a function of mass number. The thick solid line represents the main component obtained by means of the classical model and the thin line corresponds to the weak component in massive stars (see text). Symbols denote the empirical products for the *s*-only nuclei. Some important branchings of the neutron capture chain are indicated as well.

and ^{82}Kr, although the terrestrial (ground state) half-life of ^{79}Se is about 10^5 years.

The lack of reliable stellar (n, γ) rates was clearly felt by B^{2}FH, who emphasized that 'unambiguous results would be obtained by measuring the total absorption cross sections, but it is very difficult experimentally. It is our view, however, that such measurements would serve as a crucial test of the validity of the *s* process.'

In this paper the status of the stellar (n, γ) rates for the isotopes on the *s*-process path is summarized in Section 2. The theoretical aspects, which have to be considered in the transition from laboratory measurements to stellar applications, are discussed in Section 3. Apart from the fact that many cross sections of the stable isotopes are still rather uncertain and need to be improved, the main challenge of future experiments is to extend such measurements to the largely unexplored subset of unstable branch point nuclei (Section 4). This section covers also the possibility to complement (n, γ) experiments by studies of the inverse (γ, n) reactions and includes the related problems of stellar β-decay rates as well. Current improvements in experimental techniques and by the construction of new, more intense neutron facilities are addressed in Section 5 and the resulting possibilities are eventually sketched in Section 6.

2 Status of Experimental (n, γ) Cross Sections

A first compilation of stellar neutron capture cross sections was published by Allen et al. (1971). In this paper the role of neutron capture reactions for the nucleosynthesis of heavy elements was reviewed and a list of recommended (experimental or semi-empirical) Maxwellian averaged cross sections (MACS) at $kT = 30$ keV was presented for nuclei between C and Pu.

The idea of an experimental and theoretical stellar neutron cross section database for *s*-process studies was picked up 16 years later by Bao and Käppeler (1987). This compilation included cross sections for (n, γ) reactions between ^{12}C and ^{209}Bi, some (n, p) and (n, α) reactions (from ^{33}Se to ^{59}Ni) and also (n, γ) and (n, f) reactions for long-lived actinides. A follow-up compilation was published 5 years later by Beer et al. (1992).

In the last update in 2000, the compilation of Bao et al. (2000) was extended down to ^{1}H and included – as in the paper by Allen et al. (1971) – semi-empirical recommended values for nuclides without experimental cross section information. These estimated values are cross sections derived with the Hauser-Feshbach code NON-SMOKER (Rauscher & Thielmann 2000), which are corrected for known systematic deficiencies in the nuclear input of the calculation. Additionally, the database provided stellar enhancement factors and energy-dependent MACS for energies between $kT = 5$ and 100 keV.

The KADONIS project (Dillmann et al. 2005) is based on these previous compilations and is intended as a regularly updated database. It has been available online[3] since April 2005. The current version KADONIS v0.2 (January 2007) is already the second update and includes – compared to the compilation of Bao et al. (2000) – recommended values for 38 improved and 14 new cross sections. In total, data sets are available for 353 isotopes, including 76 radioactive nuclei (22%) on or close to the *s*-process path. For 12 of these radioactive nuclei, experimental data is available, i.e. for ^{14}C, ^{93}Zr, ^{99}Tc, ^{107}Pd, ^{129}I, ^{135}Cs, ^{147}Pm, ^{151}Sm, ^{154}Eu, ^{163}Ho, ^{182}Hf and ^{185}W. The remaining 64 radioactive nuclei are not (yet) measured in the stellar energy range and are represented only by semi-empirical cross section estimates with typical uncertainties of 25 to 30%. Almost all of the (n, γ) cross sections of the 277 stable isotopes have been measured. The few exceptions ^{36,38}Ar, ^{40}K, ^{50}V, ^{72,73}Ge, ^{77}Se, ^{98,99}Ru, ^{131}Xe, ^{138}La and ^{195}Pt lie partly outside the *s*-process path in the proton-rich *p*-process domain. Most of these cross sections are difficult to determine because they are not accessible by activation measurements or because samples are not available in sufficient amounts and/or enrichment for time-of-flight measurements.

2.1 Recent Improvements

The compilation of Bao et al. (2000) included also 31 *p*-process nuclei between ^{74}Se and ^{196}Hg, which could be produced by the *s* process in minor amounts (with exception of the pure *p*-process isotope ^{138}La). These stable, proton-rich nuclei are 10–100 times less abundant than their neighboring *s*- and *r*-process isotopes. The preferred astrophysical site and mechanism for the production of the largest fraction of *p* nuclei is the γ process in explosive O/Ne burning during core collapse supernovae (Arnould & Goriely 2003) and in the *νp* process near the surface of the nascent neutron star (Fröhlich et al. 2006), with possible contributions from the *rp* process due to explosive hydrogen burning on accreting neutron stars (Schatz et al. 1998).

[3] `http://nuclear-astrophysics.fzk.de/kadonis`

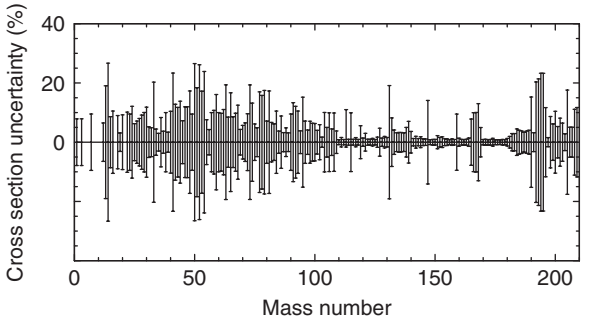

Figure 2 Present uncertainties of the stellar (n, γ) cross sections required for *s*-process nucleosynthesis. These values refer to a thermal energy of $kT = 30$ keV, but may be considerably larger at lower and higher temperatures.

The most important reactions in the γ process are (γ, n) reactions on pre-existing seed nuclei. Since direct (γ, n) measurements are up to now restricted to a few cases such as ^{190}Pt (Vogt et al. 2001) and ^{196}Hg (Sonnabend et al. 2004), the main information on these reaction comes from (n, γ) cross section measurements, which can be converted into the respective inverse reaction channel via detailed balance. For the 32 stable *p* nuclei such measurements existed only for 20 isotopes, almost half of them with uncertainties >9%. This motivated an extended activation campaign at the Karlsruhe 3.7 MV Van de Graaff accelerator using stellar neutron spectra for $kT = 25$ keV produced by the ^{7}Li$(p, n)^{7}$Be reaction. By end of 2007 only ^{98}Ru and ^{138}La will remain unmeasured, because neutron capture on these isotopes leads to stable neighbors. Since 2002, theoretical predictions for the cross sections of ^{74}Se, ^{84}Sr, ^{102}Pd, ^{120}Te, ^{132}Ba, ^{158}Dy, ^{168}Yb, ^{174}Hf, ^{184}Os and ^{196}Hg were already replaced by experimental data (Dillmann et al., in preparation).

The actual status of the cross sections required for *s*-process nucleosynthesis calculations is summarized in Figure 2, showing the respective uncertainties as a function of mass number. Though the necessary uncertainties of 1–5% have been locally achieved, further improvements are clearly required, especially in the mass region below $A = 120$ and above $A = 180$, where the desired accuracy is far from being reached. Future efforts in this field are the more important as Figure 2 reflects the situation for a thermal energy of 30 keV. In most cases, however, extrapolation to lower and higher temperatures implies still larger uncertainties.

2.2 Extensions of KADONIS

The present version of KADONIS consists of two parts: the *s*-process library and a collection of available experimental *p*-process reactions. The *s*-process library will be complemented in the near future by some (n, p) and (n, α) cross sections measured at $kT = 30$ keV, as it was already included in Bao & Käppeler (1987). The *p*-process database will be a collection of all available charged-particle reactions measured within or close to the Gamow window of the *p* process ($T_9 = 2$–3 GK).

A further extension of KADONIS is planned to include more radioactive isotopes, which are relevant for *s*-process nucleosynthesis at higher neutron densities (up to 10^{11} cm^{-3}) (Cristallo et al. 2006). Since these isotopes are more than one atomic mass unit away from the 'regular' *s*-process path on the neutron-rich side of stability, their stellar (n, γ) values have to be extrapolated from known cross sections by means of the statistical Hauser–Feshbach model. The present list covers 73 new isotopes and is available on the KADONIS homepage.

3 Status of Theory

Theoretical modeling of the neutron capture reaction rates as well as of other reaction channels is necessary in several respects. As already pointed out in the previous sections, measurements cannot be performed at all energies and for all relevant isotopes. In addition, the reaction rates in a stellar environment require estimation of reaction processes for nuclei in their excited states, which cannot be directly measured under laboratory conditions.

The key reaction model around which most of the rates necessary for *s*-process studies is based on the Hauser-Feshbach statistical model theory (HFSM). In its complete formulation and critical evaluation, the HFSM has been around for over 30 years (Moldauer 1975). The model relies essentially on two basic assumptions: (a) the compound nucleus reaction mechanisms and (b) a statistical distribution of nuclear excited states. Adopting these assumptions, the reaction cross section (e.g. for neutron capture) can be written in terms of model parameters such as the energy-dependent neutron transmission functions $T_{n,ls}$ and the γ-ray transmission functions $T_{\gamma,J}$. The general expression reads

$$\sigma_{n,\gamma}(E_n) = \frac{\pi}{k_n^2} \sum_{J,\pi} g_J \frac{\sum_{ls} T_{n,ls} T_{\gamma,J}}{\sum_{ls} T_{n,ls} + \sum_{n,ls} T_{n',ls} + T_{\gamma,J}} W_{\gamma,J} \tag{1}$$

where E_n is the incident neutron energy, k_n the wave number, $s = 1/2$ the incident particle intrinsic spin and l the orbital angular momentum of the neutron-nucleus relative motion. $g_J = (2J + 1)(2s + 1)^{-1}(2I + 1)^{-1}$ is a statistical weighting factor for target nuclei of spin I and compound states of total angular momentum J and parity π compatible with spin and parity conservation laws. W_γ is a factor, which takes into account the different statistical fluctuation properties of the γ-decay channel as compared to the neutron elastic (n) and inelastic (n') channels. The various nuclear quantities mentioned can be calculated using different nuclear structure and de-excitation models. It is here that the various HFSM approaches used so far differ among each other.

Examples of widely used approaches to the HFSM parameterization for applications in nuclear astrophysics are those of Holmes et al. (1976) and Harris (1981) as well as the latest 'NON-SMOKER' (Rauscher & Thielemann 2001), 'MOST' (Arnould & Goriely 2006) and 'TALYS'

(Koning et al. 2005) versions. Most of the quoted references include also HFSM computer codes for calculation of reaction cross sections. A repository of parameters and systematics of nuclear structure quantities can be found in the 'RIPL' initiative[4]. Additional model codes have been used for individual reaction rate calculations.

3.1 Stellar Enhancement Factors

The reaction processes under stellar conditions must consider the thermal population of excited nuclear states. Capture rates in particular may be affected by this process. The capture cross section from excited states can be modeled as for ground states. There is, however, the possibility to have additional inelastic scattering channels from reactions on excited states. In particular, the so-called 'super-elastic' channel, in which the incident neutron leads to a lower state in the target, is a particularly relevant process. In the HFSM equation reported above, this means that the transmission coefficients for the inelastic channels, $T_{n',ls}$, must take into account the open super-elastic channels. A good benchmark of the neutron-nucleus interaction used to calculate the transmission functions related to this process can be provided by a measurement of the inelastic scattering cross section and by its comparison with the model calculation.

The compound nuclear states formed by the capture from excited states are the same (except for total angular momentum) as those excited from the ground-state: a consequence of the assumed compound reaction mechanism. If the modelling of the reaction process for the ground-state can be tested against a capture cross section measured in the laboratory, these constraints can reduce, at least in principle, the uncertainty of the evaluated stellar cross sections. In practice, these processes are taken into account by the so-called stellar enhancement factor (SEF), defined simply as $\langle\sigma\rangle^* = \mathrm{SEF} \cdot \langle\sigma\rangle^{\mathrm{lab}}$, where the $*$ and 'lab' indicate the stellar MACS (i.e. averaged over a population of excited states) and laboratory (ground-state) cross sections, respectively.

An important example of the situation just described is the case of the MACS of the two *s*-only isotopes ^{186}Os and ^{187}Os. Their MACS are the key ingredient for the Re/Os nuclear cosmo-chronology (Clayton 1964) and the stellar cross sections are strongly influenced by the presence of low-lying excited states, in particular in ^{187}Os (Woosley & Fowler 1979). We will show here the SEF calculation for this isotope as an example.

The calculations have been made using a HFSM code with model parameters tuned to reproduce experimental information recently derived from a neutron capture cross section measurement performed at the CERN n_TOF facility (Mosconi et al. 2006, 2007). Details of the measurements and data analysis are given in the cited references. In this particular calculation, focus is put on the presence of an excited state in ^{187}Os at 117 keV. This state has been reported only in a single measurement using the (d, t) reaction (Morgen et al. 1973), but its spin and parity assignments are still unknown. Therefore, SEF calculations were performed with all possible J-assignment for values from $1/2$ to $9/2$. The results are shown in Figure 3. At $kT = 30$ keV, the SEF corrections are rather small, while the presence of that particular state can alter the SEF considerably at higher thermal energies. The corresponding uncertainties are estimated to increase from 1 up to 3%.

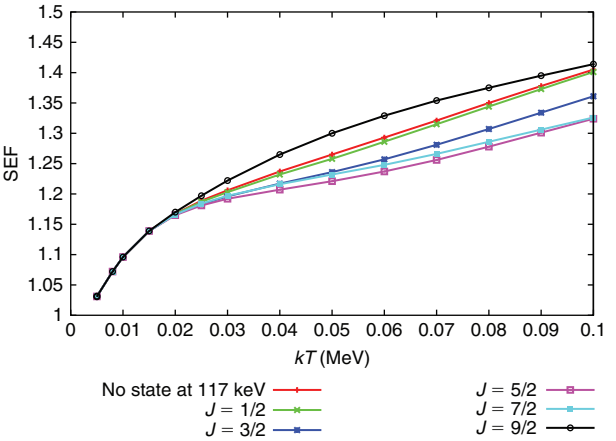

Figure 3 Stellar enhancement factor (SEF) for the ^{187}Os$(n, \gamma)^{188}$Os neutron capture reaction. The first ten excited states in ^{187}Os, up to an excitation energy of 260 keV, have been included in the calculation. The different results refer to calculations, in which the state at 117 keV is included with different spin assignments. For other details see text.

It is interesting to analyze the implications of this type of uncertainties on the galactic age (or on the duration of nucleosynthesis) using the simple model proposed by Fowler and quoted in Browne & Berman (1981). The impact of the uncertainties in the relevant quantitites of the model on the galactic age are summarized in Table 1.

Note that, associated to the SEF-30 of ^{187}Os, we have used an uncertainty of 4%. This value, which is higher than the value due to the uncertainty derived from the properties of the state at 117 keV mentioned above, takes the uncertainties of other model parameters into account as well. For example, the difference between calculations using a spherical and a deformed optical model potential for the neutron-nucleus interaction has been adopted as a contribution to the overall uncertainty of the SEF value. From variations of this kind, we estimate a typical uncertainty of ≈4–5% for the SEF calculations, if the capture cross section for the ground-state (lab) are known with sufficient accuracy and if the other model parameters in HFSM calculations can be fixed by measured quantities.

4 Problem of Unstable Isotopes

4.1 (n, γ) Measurements

As outlined above, most of the missing experimental information on stellar (n, γ) cross sections refers to unstable

[4] http://www-nds.iaea.org/RIPL-2

Table 1. Various components of the uncertainty on the nucleosynthesis time-duration (age) based on the Re/Os clock, from abundances and from nuclear data input

Quantity	Value	Uncertainty on age [Gyr]	Comment	Reference
$^{186}Os/^{187}Re$	0.2845 ± 0.0071	0.98	Abundance	Fästermann (1998)
$^{187}Os/^{187}Re$	0.2254 ± 0.0057		Abundance	Fästermann (1998)
$t_{1/2}$ [Gyr]	41.2 ± 1.12	0.56	^{187}Re β-decay	Galeazzi et al. (2001)
R_σ	0.424 ± 0.022	0.82	MACS ratio (lab)	Mosconi (2007)
SEF-30 (^{186}Os)[a]	1.03 ± 0.01	0.16	At 30 keV	Present
SEF-30 (^{187}Os)[a]	1.25 ± 0.05	0.63		
Combined total uncertainty		1.55		

[a]Including effect of all excited states and uncertainties of model calculations.

isotopes. The main difficulty in such measurements is clearly associated with the γ-activity of the sample, which restricts the amount of sample material that can be used in a measurement. Therefore, experiments with unstable samples are presently limited to cases where the specific γ-activity is rather low. A second problem in this context is the production of sufficiently large and sufficiently clean samples.

The specific γ-activity is particularly difficult to suppress in measurements with liquid scintillators, for example with C_6D_6 detectors, because their poor energy resolution prevents the discrimination via pulse height analysis. Since the time of flight (TOF) technique is the only way of reducing the γ-background, these detectors can be applied only in cases of low specific activity. An example of such a measurement is the determination of the ^{151}Sm(n, γ) cross section performed by the n_TOF collaboration (Abbondanno et al. 2004a; Marrone et al. 2006). This measurement took also advantage of the very low duty factor and unique luminosity of the n_TOF facility (Section 5.5).

HPGe detectors represent an alternative in terms of energy resolution, but the difficulties in this case arise from the low peak efficiency. Consequently, the application of HPGe detectors appears to be useful only in cross section measurements on light isotopes, where the level scheme is comparably simple and well known, so that spectroscopy of the transitions between low lying states and the ground state in the reaction product can be used for the identification of capture events. In measurements on unstable samples, HPGe detectors are further handicapped by their comparably large dead times.

The problems with C_6D_6 and HPGe detectors are to some extent avoided by the use of 4π BaF_2 arrays. In these highly segmented total absorption calorimeters the γ-background is distributed over many modules, thus reducing the dead time problem significantly. The intrinsic resolution in γ-ray energy of these detectors is important for discrimination of true capture events, which are characterised by capture cascades with sum energies defined by the binding energy of the captured neutron (ranging from typically 5 to 10 MeV), from the γ-activity of the sample, which is normally limited to energies below 1 MeV. Moreover, the nearly 100% cascade efficiency of these arrays allows one to use much smaller sample masses than with other detectors.

Apart from a measurement on ^{151}Sm (Wisshak et al. 2006a), measurements on unstable samples with such detector arrays have, so far, concentrated on the actinide region, but these examples showed that this technique can be successfully applied to unstable isotopes in general. As reported by the DANCE group, it was possible to perform a measurement with a sample of only 0.44 mg of ^{237}Np, the smallest sample ever used in an accelerator based TOF measurement of an (n, γ) cross section (Haight, in preparation). In a similar experiment, the n_TOF collaboration obtained high-resolution data with a sample of 44 mg of ^{237}Np (Guerrero et al., in preparation).

Future improvements of the neutron flux (see Section 5.5) will allow to reduce the sample mass even further. This reduction is crucial, because the intensities at future radioactive ion beam facilities will be high enough to produce such samples within a few hours with the required mass and purity.

Though applied first in the actinide region, the DANCE group is planning to use this technique to determine the (n, γ) cross sections of *s*-process branch points in the Sm–Eu–Gd region as well (Couture & Reifarth 2007).

4.2 (γ, n*) Studies*

However, there are also cases where it is not possible to measure the (n, γ) cross sections with currently available facilities and detector arrays. If the half-life of a branching point is in the order of several dozens of days, direct measurements are hindered by the preparation of an appropriate amount of sample material. If the product of the (n, γ) reaction is a stable nucleus as, for example for the branching points ^{95}Zr, ^{151}Sm and ^{185}W, it is possible to learn about the capture reaction from a measurement of the inverse photo-dissociation reaction.

In these cases the aim is not to measure the neutron capture cross section but to provide constraints on its prediction in the framework of Hauser–Feshbach theory. Differences in predicted cross sections are mainly caused

by differences in the input parameters to the theoretical model, such as the γ-ray strength function, the level density and the neutron–nucleus optical potential (Rauscher & Thielemann 2001) (Section 3).

The cross sections of the (n, γ) and (γ, n) reactions are connected via the principle of detailed balance. Therefore, a set of parameters describing the photo-dissociation data should also yield a reliable prediction of the neutron capture cross section (Sonnabend et al. 2003).

This approach is limited by the fact that one does not measure the same transition matrix elements in a photo-dissociation experiment that are used in the prediction of the (n, γ) cross section. A translation of the results for the (γ, n) reaction is only possible if the levels involved in both directions have the same characteristics.

The levels contributing to the photo-dissociation reaction have to fulfill the following equations concerning their spin and parity quantum numbers J and π:

$$J^{\pi}({}^{A}Z) \otimes J^{\pi}(\gamma) = J^{\pi}({}^{A}Z^{*}) \quad \text{and}$$
$$J^{\pi}({}^{A}Z^{*}) = J^{\pi}({}^{A-1}Z^{(*)}) \otimes J^{\pi}(n) \otimes L \qquad (2)$$

with the target nucleus ${}^{A}Z$, the compound nucleus ${}^{A}Z^{*}$ and the reaction product ${}^{A-1}Z$, respectively, and L being the angular momentum of the emitted neutron n.

The observation of a photo-dissociation reaction can be realized in a direct measurement with the outgoing neutrons being counted or a photo-activation experiment where the cross section is derived from the off-line counting of the produced unstable isotopes. In the case of (γ, n) reactions it depends on the photon source, which kind of experiment can be performed.

Continuous-energy bremsstrahlung can be produced by fully stopping a mono-energetic electron beam with energy $E_{\max}$ in a radiator target. At the High Intensity Photon Setup (HIPS) of the S–DALINAC, Darmstadt (Richter 2000; Mohr et al. 1999) and at the ELBE facility at Forschungszentrum Dresden (Erhard et al. 2006) intense brems-strahlung spectra of up to several 10^7 photons $\mathrm{keV}^{-1}\mathrm{s}^{-1}\mathrm{cm}^{-2}$ are obtained. The cross section cannot be derived directly from the activation yield,

$$Y = N_{\mathrm{target}} \int_{S_n}^{E_{\max}} \sigma(E) N_{\gamma}(E, E_{\max}) \mathrm{d}E, \qquad (3)$$

where N_{target} is the number of sample atoms, $N_{\gamma}(E, E_{\max})$ the photon intensity, S_n the neutron separation energy and $\sigma(E)$ the energy-dependent cross section of the (γ, n) reaction.

The advantage of this method is its high sensitivity due to the off-line determination of the activation yield using γ spectroscopy. Therefore, natural samples can be used so that several isotopes can be observed simultaneously. Moreover, the high photon intensities as well as the low amount of sample material needed allows one to activate several targets in one measurement and to determine the activation yields subsequently. Thus, this method is well suited for systematic studies in a broad mass range.

If the (γ, n) cross section is used to constrain the theoretical prediction of the (n, γ) cross section of a branching point, quasi-monoenergetic photon beams from Laser Compton Backscattering facilities, for example AIST at Tsukuba, Japan (Ohgaki et al. 1991) or HIγS at Duke University, Durham, USA (Weller & Ahmed 2003) can be used alternatively. Though the photon spectra at these facilities cover a much smaller energy range compared to continuous-energy bremsstrahlung, they still exhibit a width of typically 100 keV, so that the cross section can be determined with a resolution of about 100 keV only.

Due to the lower photon intensities the outgoing neutrons are measured at AIST to determine the cross section so that enriched target material is mandatory. There are several cases where both methods were applied. The resulting neutron capture cross sections were in good agreement considering the uncertainties of the experiments as well as of the theoretical predictions, for example ^{185}W (Sonnabend et al. 2003; Mohr et al. 2004) and ^{186}Re (Müller et al. 2006; Shizuma et al. 2005).

However, it would be preferable to measure the energy dependence of the photo-dissociation cross section with better resolution, especially in the astrophysically relevant region directly above the reaction threshold of the (γ, n) reactions. To realise this aim tagged photons can be used. The NEPTUN tagger setup (Lindenberg 2007) that is constructed at the S–DALINAC will be suitable for high resolution studies (25 keV at a photon energy of 10 MeV) of astrophysically relevant cross sections. The photon intensity at this setup will be comparable to the Laser Compton Backscattering facilities (about 10^4 photons $\mathrm{keV}^{-1}\mathrm{s}^{-1}$).

The emitted neutrons will be measured with an array of fourteen standard liquid scintillator detectors amended by eight ^{10}B loaded liquid scintillator detectors suited for neutron-to-photon discrimination down to low neutron energies. While the energy of the neutron is determined via time-of-flight, its angular momentum can be derived from the measured angular distribution. The improved energy resolution will thus allow one to distinguish between transitions to the ground state and excited states in the product nucleus. Accordingly, the cross section corresponding to selected transition matrix elements will become measurable in some unique cases.

4.3 Beta Decay Rates

A detailed evaluation of beta decay rates for *s*-process analyses has been presented by Takahashi and Yokoi (1987) on the basis of a thorough classification of possible contributions from thermally excited states and by considering the relevant effects related to the high degree of ionization in the stellar plasma. The most spectacular consequence of ionization is the enormous enhancement of decays with small Q_{β} values, where the decay electrons can be emitted into unoccupied atomic orbits. This bound beta decay was eventually confirmed in storage ring experiments with fully stripped ^{163}Ho and ^{187}Re

atoms at GSI Darmstadt, Germany (Jung et al. 1992; Bosch et al. 1996).

The quantitative assessment of the temperature dependent decay rates of the key branch point isotopes requires more experimental information on log ft values for the decay of excited states as well as more storage ring experiments to expand our knowledge of bound beta decay rates. Experimental possibilities have been discussed in Käppeler (1999), but must be extended by the successful recent application of $(d,^2\mathrm{He})$ reactions (Frekers 2005).

5 Improvements in Experimental Techniques

5.1 Differential Methods: Detectors and Techniques

The aim of the so-called differential methods is to determine the neutron capture cross section versus neutron energy. From these data, MACSs can be determined for any stellar temperature of interest. The differential methods are based on the time-of-flight technique and require pulsed neutron sources (Section 5.5). Recent developments and improvements in both neutron sources and detection techniques have led to (n, γ) cross section measurements with improved accuracy, in many cases with uncertainties of a few percent. This progress is essential for obtaining the *s* abundances with sufficient accuracy to infer the physical conditions at the stellar site of the *s* process from the observed isotope patterns in solar material and in presolar grains.

The sum of the γ-ray cascade emitted in the decay of the compound nucleus represents the best signature of a capture event. Hence, 4π detectors with an efficiency close to 100% are the most direct way to unambiguously identify (n, γ) reactions and to determine capture cross sections. This calorimetric approach started with the use of large liquid scintillator tanks, which are meanwhile replaced by arrays consisting of BaF_2 crystals because of their superior resolution in γ-ray energy and correspondingly lower backgrounds. A detector of this type consisting of 42 modules was developed at Karlsruhe (Wisshak et al. 1990) and is also in use at the n_TOF facility at CERN (Heil 2001). In this design the BaF_2 crystals are shaped as truncated pyramids, forming a fullerene-type geometry where each module covers the same solid angle. A somewhat simpler approach was chosen at ORNL (Guber et al. 1997), where 12 hexagonal BaF_2 detectors are surrounding the sample in a cylindrical geometry.

Recent examples of accurate cross section measurements made with the Karlsruhe 4π detector comprise the unstable branch point isotope ^{151}Sm (Wisshak et al. 2006a) and the Lu- and Hf-isotopes (Wisshak et al. 2006b,c). These results are essential for constraining the temperature at the *s*-process site via the branchings at $A = 151$, 175 and 179.

The segmentation of a 4π detector array is of particular advantage for separating true capture events from backgrounds. The state-of-the-art in this respect is the DANCE array with 162 BaF_2 modules that is operated at LANSCE (Reifarth et al. 2004).

The high efficiency of 4π arrays in combination with intense pulsed neutron sources provides the possibility for measurements on very small samples. In particular, this is important for radioactive isotopes, where the background from the activity of the sample needs to be kept at a minimum, and for materials in general, where only small quantities are available. A detailed survey for future measurements of neutron capture cross sections on radioactive isotopes, with special emphasis on branching points along the *s*-process path, is given in Couture & Reifarth (2007).

The main problem in using 4π arrays arises from their response to neutrons scattered in the sample. Although the scintillator is selected to consist of nuclei with small (n, γ) cross sections, about 10% of the scattered neutrons are captured in the scintillator. The resulting background is attenuated by an absorber shell around the sample, which consists of ^{6}LiH (Reifarth et al. 2004) or of a ^{6}Li containing compound (Heil 2001). Such an absorber is not required in the setup at Karlsruhe because the neutron spectrum is limited to energies below 225 keV, which allows one to separate the background from sample scattered neutrons via TOF.

This type of background becomes prohibitive for measurements on neutron magic nuclei and on light isotopes with small capture cross sections, where the neutron scattering channel is orders of magnitude stronger. Therefore, large detector arrays can not be used for these cross sections, which are of fundamental importance because they act as bottlenecks in the *s*-process path or as potential neutron poisons.

This problem was first addressed by the development of Moxon–Rae type detectors (Moxon & Rae 1963). By the design of this type it was ensured that the γ-ray efficiency is almost proportional to the energy deposited in the detector. In this way, the detection probability for capture events becomes independent of the cascade multiplicity or of the details of the pulse height spectrum.

In order to improve the very small efficiency of Moxon–Rae detectors, this solution was generalized by the idea of the Pulse Height Weighting Technique (PHWT) (Macklin & Gibbons 1967), where the proportionality between deposited energy and γ-ray efficiency is achieved a posteriori by an off-line weighting function applied to the detector response.

The PHWT technique was first applied to detectors using C_6F_6 liquid scintillators because of the smaller neutron sensitivity compared to scintillators containing hydrogen. However, the background due to scattered neutrons turned out to remain rather large, resulting in large systematic uncertainties as illustrated by the examples given in Koehler et al. (2000) and Guber et al. (2005a,b).

This problem could be reduced in a second generation of detectors, which are based on deuterated benzene (C_6D_6) because of the smaller capture cross section of deuterium. Further improvement was achieved by minimizing

the construction materials and by replacing aluminum and steel by graphite or carbon fibre, resulting in a solution, where the background due to scattered neutrons is practically negligible (see e.g. Plag et al. 2003; Koehler et al. 2000).

The accuracy of the PHWT has been an issue for a long time. When the technique was proposed, the uncertainties introduced by the Weighting Functions (WFs) were about 20% in some particular cases (Macklin 1987). Dedicated measurements and Monte Carlo (MC) calculations (Corvi et al. 1988; Perey et al. 1988) have led to gradually improved WFs. With present advanced MC codes, realistic detector response functions and WFs could be determined using precise and detailed computer models of the experimental setups (Koehler 1996; Tain et al. 2002; Abbondanno 2004; Borella et al. 2005). A dedicated set of measurements at the n_TOF facility confirmed that WFs obtained by the refined simulations allows one to determine neutron capture cross sections with a systematic accuracy of better than 2% (Abbondanno 2004).

5.2 New Data Acquisition Systems

Modern electronic techniques have led to substantial improvements in data acquisition and storage. Flash analog-to-digital converters (FADCs) are, at present, the fastest and safest way to store and analyze analogue signals. With this technique it is possible to digitise the entire wave-form of the detector signals, instead of recording only their amplitude or integrated charge. To acquire and store the raw information has several advantages. On one hand, recording all detector signals during a measurement allows for a rigorous assessment of uncertainties related with the performance of the detectors. Distortions in the raw data such as baseline shifts, pileup and noise are efficiently identified and corrected during data analysis. The relevant parameters of the electronic signals such as time information, amplitude, area, etc., are determined off-line via pulse shape analysis (PSA) algorithms specifically designed for each type of detector. In case that these algorithms are improved at some point, one can always access the original raw information and extract more precise parameters from the same experiment.

Using FADCs to acquire data, accidental errors related with the failure of an electronic module are minimised, simply because there are much less electronic devices between the detector and the final storage, thus allowing in general to run the measurement under more stable conditions. For example, the anode signal of a photomultiplier is simply plugged into an FADC-channel, which is then read by a computer.

In this way, background sources can be better identified and corrected, particularly in the case of measurements performed with 4π BaF_2 arrays. Using FADCs there is more flexibility to develop algorithms, which allow one to discriminate contaminant neutron capture events in the scintillator via n/γ-identification (Marrone et al. 2006b) and also to discriminate the intrinsic background arising from the internal α- or β-activity in BaF_2 scintillators (Reifarth et al. 2004).

Combined with an appropriate time structure of the neutron beam, FADCs allow one to practically avoid dead-times in an experiment, even with very high count rates. A good example is the data acquisition system at n_TOF (Abbondanno et al. 2005). At this facility, data peak rates of up to 8 Mbyte per burst and per detector can be reached due to the very high instantaneous neutron flux of 10^6 n/bunch. The low pulse repetition rate of $\sim$0.4 Hz leaves enough time to digitise and store all the raw FADC information after every neutron bunch and for all detectors employed. This optimal situation leads to an almost dead-time free data acquisition process, except for cases when two consecutive signals occur too close in time to be distinguished as independent events. This can lead to a small pileup 'dead-time' of 15–20 ns.

The acquisition system at n_TOF is based on 8-bit FADC modules, with sampling rates up to 2 GHz and 8 or 16 Mbyte memory. The sampling rate is adjusted for each channel or detector in such a way, that the electronic signals are recorded with enough time resolution. Frequencies of 500 MHz are commonly used for sampling the signals of both C_6D_6 and BaF_2 detectors. The main drawback of a FADC-based acquisition system is the huge amount of accumulated data, which demands large storage capabilities and high data transfer rates. This difficulty can be mitigated by applying a zero suppression algorithm on the fly (Abbondanno et al. 2005).

5.3 Activation Method

Since it was found that stellar neutron spectra can be produced in the laboratory, the activation method has been used extensively in MACS measurements. So far, three reactions have been invoked for this technique. The ^{7}Li$(p, n)^7$Be reaction yields a quasi-stellar spectrum for a thermal energy of $kT = 25$ keV (Beer & Käppeler 1980; Ratynski & Käppeler 1988) very close to the 23 keV effective thermal energy in He shell flashes of low mass AGB stars, where neutrons are produced via the ^{22}Ne$(\alpha, n)^{25}$Mg reaction. The main neutron source in these stars, the ^{13}C$(\alpha, n)^{16}$O reaction, was simulated recently by means of the ^{18}O$(p, n)^{18}$F reaction (Heil et al. 2005).

While these two quasi-stellar spectra allow one to determine the MACSs necessary for studies of the main *s* component, the weak component associated with massive stars is characterized by higher temperatures, that is 26 keV thermal energy during core He burning and about 90 keV in the shell C burning phase. The situation during core He burning is again well described by the ^{7}Li$(p, n)^7$Be reaction, but the high temperatures during shell C burning are only roughly represented by means of the ^{3}H$(p, n)^3$He reaction, which provides a spectrum for $kT = 52$ keV (Käppeler et al. 1987). In this case, the measured MACS have to be extrapolated by statistical model calculations.

The source intensities that can be presently achieved with these quasi-stellar neutron spectra are of the order of 10^9, 10^8 and 10^5 s^{-1} for the (p, n) reactions on ^{7}Li, ^{3}H and ^{18}O, respectively. These numbers are obtained by assuming a proton beam current of 100 μA on target, a value that can be reached with electrostatic accelerators. Future developments, however, will provide much higher beam currents and correspondingly higher neutron fluxes (Section 5.5).

Already at present, the neutron intensities for activation measurements exceed the fluxes obtainable in TOF measurements by orders of magnitude. For example, the highest neutron flux reached at an experimental TOF setup is obtained with 5×10^5 s^{-1} at the DANCE array in Los Alamos. Accordingly, activation represents the most sensitive method for (n, γ) measurements in the astrophysically relevant energy range. This feature is unique for the possibility to measure the MACSs of neutron poisons, abundant light isotopes with very small cross sections, as well as for the use of extremely small sample masses.

The latter aspect is most important for the determination of MACSs of unstable isotopes, where TOF measurements are challenged by the background due to the sample activity (Section 4.1). An illustrative example in this respect is the successful measurement of the MACS of ^{147}Pm, which was performed with a sample of only 28 ng in order to compensate for the short half-life of 2.6 yr (Reifarth 2003).

Another important feature of the activation method is that it is insensitive to the reaction mechanism. In particular, it includes the contributions from Direct Capture (DC), where the neutron is captured directly into a bound state. The DC component, which contributes substantially to the (n, γ) cross sections of light nuclei, is extremely difficult to determine in TOF measurements (for an exception see the specialized setup used in Igashira et al. 1995).

The advantages of coupling the activation technique with Accelerator Mass Spectrometry (AMS), which opens new applications and improvements, are outlined in the following subsection.

5.4 Determination of Cross Sections with Accelerator Mass Spectrometry

The activation technique has recently been combined with Accelerator Mass Spectrometry (AMS), an extension that provided access to previously inaccessible cases, for example to reactions producing very long-lived nuclei with very weak or completely missing γ transitions. The application of AMS counting in stellar neutron reactions has the further advantage of being independent of uncertainties in γ-ray intensities. The successful combination of the two methods has been demonstrated for a number of cases, e.g. for determination of the stellar (n, γ) cross sections of ^{9}Be, ^{13}C, ^{35}Cl, ^{40}Ca, ^{54}Fe, ^{58}Ni, ^{209}Bi and ^{235}U (Coquard, private communication; Coquard et al. 2006; Wallner et al. 2007; Dillmann et al., in preparation; Rugel et al. 2007).

Apart from these examples, the branch point isotopes ^{63}Ni and ^{79}Se are particularly important for *s*-process studies. The total (n, γ) cross section of ^{78}Se has been measured using the gas-filled analyzing magnet system (GAMS) at the Munich 14 MV tandem accelerator (Knie et al. 2000; Rugel et al. 2007; Dillmann et al. 2006). Since AMS determines the concentration ratio $N_{\rm act}/N$ of a radioisotope to a stable isotope relative to a standard of known isotopic ratio, the experimental cross section can be deduced from the total neutron flux seen by the sample,

$$\sigma = \frac{N_{\rm act}}{N} \cdot \frac{1}{\Phi_{tot}} \tag{4}$$

With this technique, the (n, γ) cross section of ^{78}Se was measured for the first time to be $\langle\sigma\rangle_{30\,\rm keV} = 60.1 \pm 9.6$ mbarn.

The measurement of the ^{62}Ni neutron capture cross section is another example for the combined use of the activation method and AMS, which is expected to solve the long-standing discussion of the '^{62}Ni problem'. This cross section is crucial for the *s*-process branching at ^{63}Ni and the following reaction flow up to mass $A \approx 90$ (see Figure 4).

Already the first TOF measurements 30 years ago (Beer & Spencer 1975; G. Walter, private communication; R. Spencer, private communication) revealed severe discrepancies, with MACS values at $kT = 30$ keV ranging between 12.5 mbarn (R. Spencer, private communication) and 35.5 mbarn (G. Walter, private communication). More recently, data between 35.4 and 45.5 mbarn were published by Rauscher & Guber (2002) and a TOF measurement was reported by Tomyo et al. (2005), which yielded 37 ± 2 mbarn. An independent experiment with the activation plus AMS technique reported $\langle\sigma\rangle_{30\,\rm keV} = 22.6 \pm 2.7$ mbarn (Nassar et al. 2005). At the same time, Rauscher and Guber revised their previous calculation to 9.7–11.2 mbarn (Rauscher & Guber 2005), thus restoring the initial confusion.

This situation stimulated a new activation with a subsequent AMS measurement using the GAMS setup in Munich (S. Walter, private communication) instead of the ATLAS facility at Argonne National Laboratory (Nassar et al. 2005) in order to obtain an independent value for the ^{62}Ni cross section.

5.5 Pulsed Neutron Sources for Measurements at Stellar Energies

At small accelerators, neutrons are produced by nuclear reactions, such as ^{7}Li$(p, n)^7$Be, with the possibility of tailoring the neutron spectrum exactly to the stellar energy range between 0.3 and ≈500 keV. The limited source strength can be compensated by low backgrounds and the use of comparably short neutron flight paths (Käppeler 1999; Nagai et al. 1991). This type of accelerators is also unique for the simulation of stellar neutron spectra used with the activation technique.

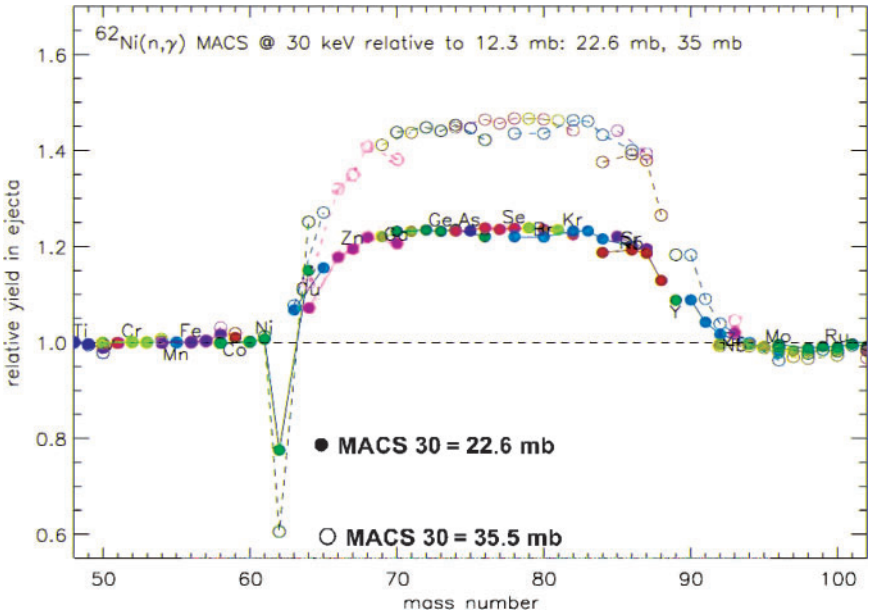

Figure 4 Influence of different ^{62}Ni cross sections on the *s*-process abundance distribution produced by the weak component in massive stars. Note that the *s*-process efficiency is significantly increasing with the stellar (n, γ) cross section of ^{62}Ni.

Much higher intensities can be achieved via (γ, n) reactions at electron linear accelerators, such as GELINA at Geel, Belgium and ORELA at Oak Ridge, USA, by bombarding heavy metal targets with electron beams of typically 50 to 100 MeV. There, background conditions are more complicated and measurements need to be carried out at larger neutron flight paths. In turn, the longer flight paths provide the possibility to study the resolved resonance region with high resolution (see for example Koehler 1996).

Spallation reactions induced by energetic particle beams constitute the most prolific pulsed sources of fast neutrons suited for TOF measurements. Presently, two such spallation sources are in operation, LANSCE at Los Alamos (Lisowski et al. 1990) and the n_TOF facility at CERN (Abbondanno et al. 2003). The main advantage of these facilities is the very efficient neutron production due to the high primary proton beam energies of 800 MeV and 20 GeV at LANSCE and n_TOF, respectively. At n_TOF, for example, 300 neutrons are produced per incident proton, which makes this facility the most luminous white neutron source presently available.

Due to their excellent efficiency, spallation sources can be operated at comparably low repetition rates while still maintaining high average intensities. The situation at LANSCE is characterised by a comparably short flight path of 20 m, a time resolution of 250 ns and a repetition rate of 50 Hz, similar to what is planned at the SNS in Oak Ridge[5] and at J-PARC in Japan[6]. The n_TOF facility at CERN represents a complementary approach aiming at higher resolution (185-m flight path, 7-ns pulse width) and even lower repetition rates of typically 0.4 Hz (Abbondanno et al. 2003).

The astrophysics options at various white neutron sources have been critically discussed by Koehler (2001) with respect to measurements using radioactive samples. This comparison shows that spallation sources are unique for their peak neutron fluxes in the astrophysically relevant keV region, but that only the n_TOF facility exhibits a neutron energy resolution comparable to that of electron linear accelerators. This is even true if the flight path at n_TOF would be reduced to 20 m. With this improvement, the performance of the n_TOF facility would be suited for TOF measurements on μg-size, radioactive samples.

A completely new approach is presently developed at the University of Frankfurt, Germany (Ratzinger et al. 2007). The Frankfurt Neutron source at the Stern-Gerlach-Zentrum (FRANZ) will provide short neutron pulses by bombardment of a ^{7}Li target with an intense proton beam. The proton energy range is limited to 2.0 ± 0.2 MeV and the pulse rate will be typically 250 kHz.

The scheme of the accelerator is sketched in Figure 5, starting with a volume-type proton source on a 150 kV high voltage platform, followed by a 100 ns chopper in the low energy beam transport line to the acceleration stage consisting of an RFQ with an exit energy of 700 keV and IH-DTL structure with an effective voltage gain of 1.4 MeV. The macro pulses at the exit contain up to 10 rf bunches, which are compressed into 1 ns pulses for neutron production in the Li target. This is achieved by a second chopper, which deflects the bunches to traces of different path length in a Mobley-type buncher system (Chau et al. 2006; Meusel et al. 2006; Ratzinger et al. 2007).

[5] http://www.sns.gov/
[6] http://j-parc.jp/

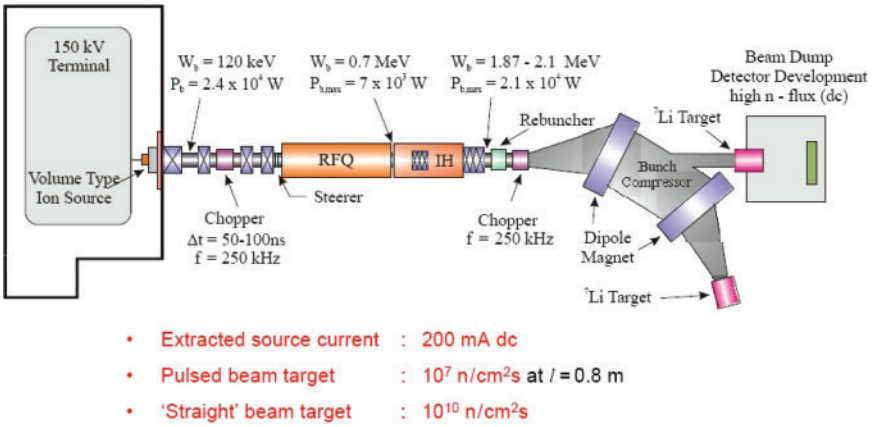

Figure 5 Schematic layout and main parameters of the Frankfurt intense neutron source (see text).

In this way, intense pulses of up to 5×10^{10} protons can be focused onto the Li target within 1 ns. The average beam current is expected to reach 2 mA, corresponding to a neutron flux of about 10^5 n cm^{-2} s^{-1} keV^{-1} at a distance of 80 cm from the target, more than an order of magnitude higher than is achieved at present spallation sources. Since the amount of sample material can be reduced by the gain in flux, TOF measurements appear to be feasible with samples of 10^{14} atoms. This number represents a breakthrough with respect to the production of unstable samples, because beam intensities of the order of 10^{10} to 10^{12} s^{-1} are expected at future Rare Isotope Facilities such as RIA (Savard 2002), RIKEN (Tanihata 1998), or FAIR[7].

Moreover, this accelerator is also perfectly suited for the simulation of stellar neutron spectra via the ^{7}Li$(p, n)^7$Be reaction (Section 5.3).

6 Future Strategies

The persisting challenges in neutron cross section data for *s*-process studies are threefold and refer to the measurement of all MACSs with the required average accuracy of $\leq$5%, the reduction of the uncertainty to 2% for the cross sections of key isotopes and the experimental determination of the cross sections of the unstable branch point nuclei.

The first goal of accurate measurements on stable isotopes can mostly be achieved by using the potential of present techniques. The performance of state-of-the-art detectors, that is optimized C_6D_6 scintillators or total absorption BaF_2 calorimeters coupled with data acquisition systems on the basis of fast digitizers allows one to reach accuracies of about 2% in most cases, in particular if planning of the experiments as well as the data analysis are performed with the MCNP and GEANT simulation tools.

The more difficult measurements of small cross sections of neutron magic nuclei and of light neutron poison isotopes will benefit from the high intensities of new neutron facilities, which will become available in the near future. With these high neutron fluxes smaller samples can be used, an essential condition for measurements on unstable samples and also for reducing the measuring times even for samples with small cross sections.

The possibility to use smaller samples has two advantages. On the one hand, this implies that isotopically pure radioactive samples can be produced by means of the intense beams at the rare isotope accelerators under construction. On the other hand, sample-related corrections are much reduced also in measurements of small cross sections, resulting in correspondingly lower systematic uncertainties.

Another aspect that will become important once higher neutron fluxes are available is that measurements can be repeated with modified experimental parameters, different detectors and even with different methods. The redundancy obtained in this way will be crucial for ensuring that corrections are properly treated and that systematic uncertainties are indeed reduced to better than 5% in general and to 1–2% for the isotopes of key importance.

[7] http://www.gsi.de/fair/reports

Acknowledgments

K.S. acknowledges support by Deutsche Forschungsgemeinschaft (SFB 634).

References

Abbondanno, U. et al., 2003, Report CERN/INTC-0-001
Abbondanno, U. et al., 2004a, PhRvL, 93, 161103
Abbondanno, U. et al., 2004b, NIMPA, 521, 454
Abbondanno, U. et al., 2005, NIMPA, 538, 692
Allen, B. J., Gibbons, J. H. & Macklin, R. L., 1971, AdNuP, 4, 205
Arlandini, C., Käppeler, F., Wisshak, K., Gallino, R., Lugaro, M., Busso, M. & Straniero, O., 1999, ApJ, 525, 886
Arnould, M. & Goriely, S., 2003, PhR, 384, 1
Arnould, M. & Goriely, S., 2006 NuPhA, 777, 157
Bao, Z. & Käppeler, F., 1987, ADNDT, 36, 411
Bao, Z. et al., 2000, ADNDT, 76, 70
Beer, H. & Käppeler, F., 1980, PhRvC, 21, 534
Beer, H. & Spencer, R., 1975, NucPhA, 240, 29
Beer, H., Voß, F. & Winters, R., 1992, ApJS, 80, 403

Borella, A. et al., 2005, in AIPC 769, International Conference on Nuclear Data for Science and Technology, 652
Bosch, F. et al., 1996, PhRvL, 77, 5190
Browne, J. C. & Berman, B. L., 1981, PhRvC, 23, 1434
Burbidge, E., Burbidge, G., Fowler, W. & Hoyle, F., 1957, RVMP, 29, 547
Cameron, A., 1957, Technical report, A.E.C.L. Chalk River, Canada
Chau, L. et al., 2006, in EPAC 2006, 1690
Clayton, D. D., 1964, ApJ, 139, 637
Coquard, L., Käppeler, F., Dillmann, I., Wallner, A., Knie, K. & Kutschera, W., 2006, in Proc. International Symposium on Nuclear Astrophysics, Nuclei in the Cosmos IX, 274
Corvi, F., Prevignano, A., Liskien, H. & Smith, P., 1988, NIMPA, 265, 475
Couture, A. & Reifarth, R., 2007, ADNDT, 93, 807
Cristallo, S., Gallino, R., Straniero, O., Piersanti, L. & Dominguez, I., 2006, MmSAI, 77, 774
Dillmann, I. et al., 2005, in AIPC 819, Capture Gamma-Ray Spectroscopy and Related Topics, Eds. Woehr, A. & Aprahamian, A. (New York, AIP), 123
Dillmann, I. et al., 2006, in Proc. International Symposium on Nuclear Astrophysics, Nuclei in the Cosmos IX, 89
Erhard, M. et al., 2006, EPJA, 27, 135
Fästermann, T., 1998, in Proc. 9th Workshop on Nuclear Astrophysics, 171
Frekers, D., 2005, NuPhA, 752, 580
Fröhlich, C. et al., 2006, PhRvL, 96, 142502
Galeazzi, M., Fontanelli, F., Gatti, F. & Vitale, S., 2001, PhRvC, 63, 014302
Gallino, R. et al., 1998, ApJ, 497, 388
Guber, K., Spencer, R., Koehler, P. & Winters, R., 1997, NuPhA, 621, 254
Guber, K. H. et al., 2005a, NIMPB, 241, 218
Guber, K. H. et al., 2005b, in AIPC 769, Nuclear Data for Science and Technology, Eds. Haight, R. C., Chadwick, M. B., Kawano, T. & Talou, P. (New York, AIP), 1706
Harris, M., 1981, Ap&SS, 77, 357
Heil, M. et al., 2001, NIMPA, 459, 229
Heil, M., Dababneh, S., Juseviciute, A., Käppeler, F. & Plag, R., 2005, PhRvC, 71, 025803
Holmes, J., Woosley, S., Fowler, W. & Zimmerman, B., 1976, ADNDT, 18, 305
Igashira, M., Nagai, Y., Masuda, K., Ohsaki, T. & Kitazawa, H., 1995, ApJ, 441, L89
Jung, M. et al., 1992, PhRvL, 69, 2164
Käppeler, F., 1999, PrPNP, 43, 419
Käppeler, F., Naqvi, A. & Al-Ohali, M., 1987, PhRvC, 62, 936
Knie, K. et al., 2000, NIMPB, 172, 717
Koehler, P. E., Spencer, R. R., Winters, R. R., Guber, K. H., Harvey, J. A., Hill, N. W. & Smith, M. S., 1996, PhRvC, 54, 1463
Koehler, P., 2001, NIMPA, 460, 352
Koehler, P. et al., 2000, PhRvC, 62, 055803
Koning, A., Hilaire, S. & Duijvestijn, M. C., 2005, in AIPC 769, International Conference on Nuclear Data for Science and Technology, 652
Limongi, M., Straniero, O. & Chieffi, A., 2000, ApJS, 129, 625
Lindenberg, K., 2007, PhD Thesis, Institut für Kernphysik, TU Darmstadt
Lisowski, P., Bowman, C., Russell, G. & Wender, S., 1990, NSE, 106, 208
Macklin, R., 1987, NSE, 95, 200
Macklin, R. & Gibbons, J., 1967, PhRv, 159, 1007
Marrone, S. et al., 2006a, PhRvC, 73, 034604
Marrone, S. et al., 2006b, NIMPA, 568, 904
Meusel, O. et al., 2006, in Linac 2006, 159
Mohr, P. et al., 1999, NIMPA, 423, 480
Mohr, P. et al., 2004, PhRvC, 69, 032801
Moldauer, P. A., 1975, PhRvC, 11, 426
Mosconi, M. et al., 2007, Proceedings of NPA3, in press
Mosconi, M. et al., 2006, in Proc. International Symposium on Nuclear Astrophysics, Nuclei in the Cosmos IX, 55
Morgen, P. et al., 1973, NuPhA, 204, 81
Moxon, M. & Rae, E., 1963, NucIM, 24, 445
Müller, S., Kretschmer, A., Sonnabend, K., Zilges, A. & Galaviz, D., 2006, PhRvC, 73, 025804
Nagai, Y. et al., 1991, ApJ, 381, 444
Nassar, H. et al., 2005, PhRvL, 94, 092504
Ohgaki, H. et al., 1991, ITNS, 38, 386
Perey, F. G. et al., 1988, in Nuclear Data for Science and Technology (Tokyo), 379
Plag, R. et al., 2003, NIMPA, 496, 425
Raiteri, C., Busso, M., Gallino, R. & Picchio, G., 1991, ApJ, 371, 665
Raiteri, C. M., Gallino, R., Busso, M., Neuberger, D. & Kaeppeler, F., 1993, ApJ, 419, 207
Ratynski, W. & Käppeler, F., 1988, PhRvC, 37, 595
Ratzinger, U. et al., in 18th Meeting of the International Collaboration on Advanced Neutron Sources
Rau, F., 1963, Nukleonik, 5, 191
Rauscher, T. & Guber, K., 2002, PhRvC, 66, 028802
Rauscher, T. & Guber, K., 2005, PhRvC, 71, 059903
Rauscher, T. & Thielemann, F.-K., 2000, ADNDT, 75, 1
Rauscher, T. & Thielemann, F.-K., 2001, ADNDT, 79, 47
Reifarth, R. et al., 2003, ApJ, 582, 1251
Reifarth, R. et al., 2004, NIMPA, 531, 530
Richter, A., 2000, PrPNP, 44, 3
Rugel, G. et al., 2007, NIMPB, 259, 683
Savard, G., 2002, APS Meeting Abstracts 5003
Schatz, H. et al., 1998, PhR, 294, 167
Shizuma, T. et al., 2005, PhRvC, 72, 025808
Sonnabend, K. et al., 2003, ApJ, 583, 506
Sonnabend, K., Vogt, K., Galaviz, D., Müller, S. & Zilges, A., 2004, PhRvC, 70, 035802
Straniero, O., Gallino, R., Busso, M., Chiefei, A., Raiteri, C. M., Limongi, M. & Salaris, M., 1995, ApJ, 440, L85
Tain, J., Gunsing, F., Cano-Ott, D. & Domingo, C., 2002, JNSTS, 2, 689
Takahashi, K. & Yokoi, K., 1987, ADNDT, 36, 375
Tomyo, A. et al., 2005, ApJ, 623, L153
Tanihata, I., 1998, JPhG, 24, 1311
Travaglio, C., Galli, D., Gallino, R., Busso, M., Ferrini, F. & Straniero, O., 1999, ApJ, 521, 691
Travaglio, C. et al., 2001, ApJ, 549, 346
Travaglio, C. et al., 2004, ApJ, 601, 864
Vogt, K. et al., 2001, PhRvC, 63, 055802
Wallner, A. et al., 2007, NIMPB, 259, 677
Weller, H. R. & Ahmed, M. W., 2003, MPLA, 18, 1569
Woosley, S. E. & Fowler, W. A., 1979, ApJ, 233, 411
Wisshak, K., Guber, K., Käppeler, F. & Voss, F., 1990, NIMPA, 299, 60
Wisshak, K. et al., 2006a, PhRvC, 73, 015802
Wisshak, K. et al., 2006b, PhRvC, 73, 015807
Wisshak, K. et al., 2006c, PhRvC, 73, 045807